

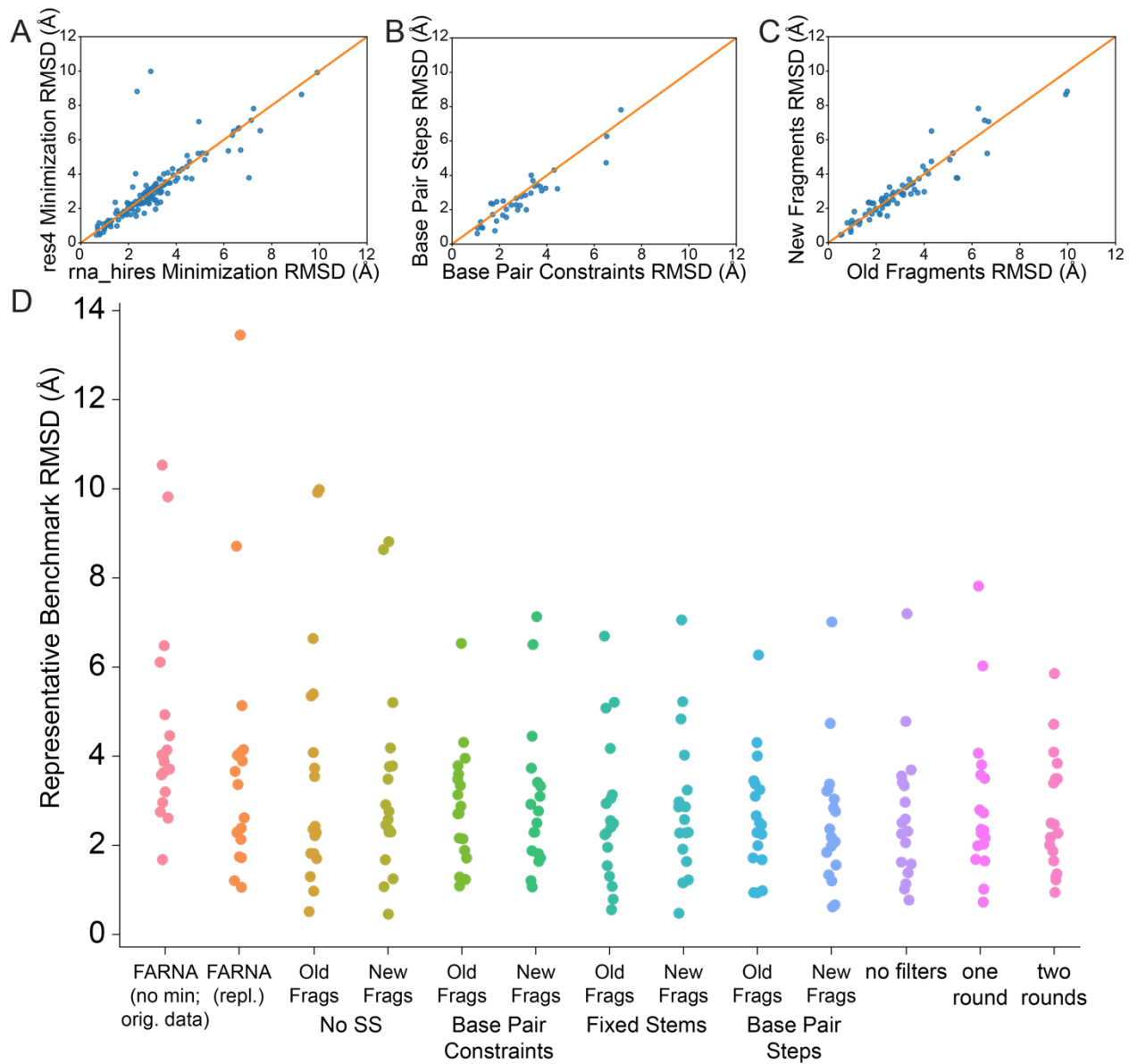
**Structure, Volume 28**

**Supplemental Information**

**FARFAR2: Improved *De Novo* Rosetta**

**Prediction of Complex Global RNA Folds**

**Andrew Martin Watkins, Ramya Rangan, and Rhiju Das**

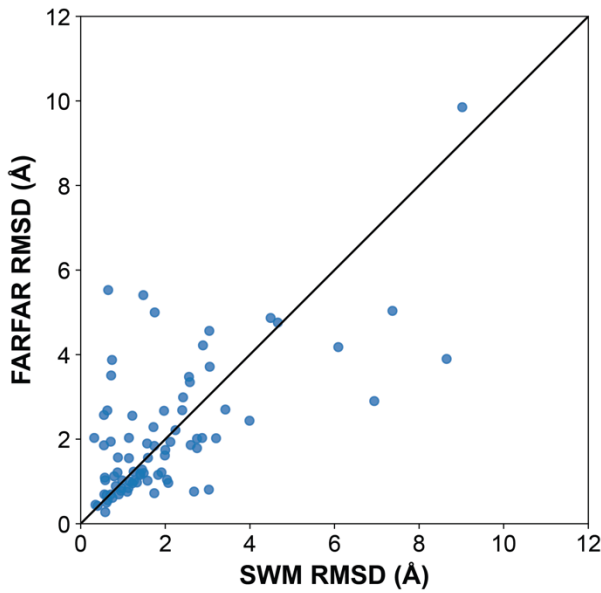


1           **Figure S1.** Related to Figure 1. FARFAR2 performance on the Classics benchmark.  
 2           We conducted many pairwise comparisons on the top-1%-RMSD values of the Classics  
 3           benchmark, where we altered only one variable between the setting chosen to define FARFAR2  
 4           and the complementary FARFAR/FARNA condition. (A) Optimization in the energy function  
 5           originally developed for SWM (y-axis) was more effective than the original FARFAR energy  
 6           function (x-axis), giving better RMSD in 91 of 144 possible comparisons. It was also  
 7           considerably more effective than no minimization at all (not shown), giving better RMSD in 102  
 8           cases, often by considerable margins. (B) Providing secondary structure information, particularly  
 9           as fixed helices or base pair steps (y-axis), offered substantial advantages over energetic  
 10

1 restraints (x-axis) or no secondary structure information. Fixed stems produced a superior RMSD  
2 in 68 of 108 possible such comparisons against other secondary structure specification methods,  
3 while base pair steps produced a superior RMSD in 76 of 108 comparisons. (C) Some benefit  
4 was also seen by using a newly obtained fragment library (y-axis) over the original FARFAR  
5 fragment library (x-axis), giving better results in 43 of 72 comparisons and providing the greatest  
6 advantage in the hardest problems. (D) A full comparison of simulation results using “res4”  
7 minimization, versus FARNA simulation and controls using the FARFAR2 simulation  
8 parameters but no filters or only one or two rounds of fragment assembly.

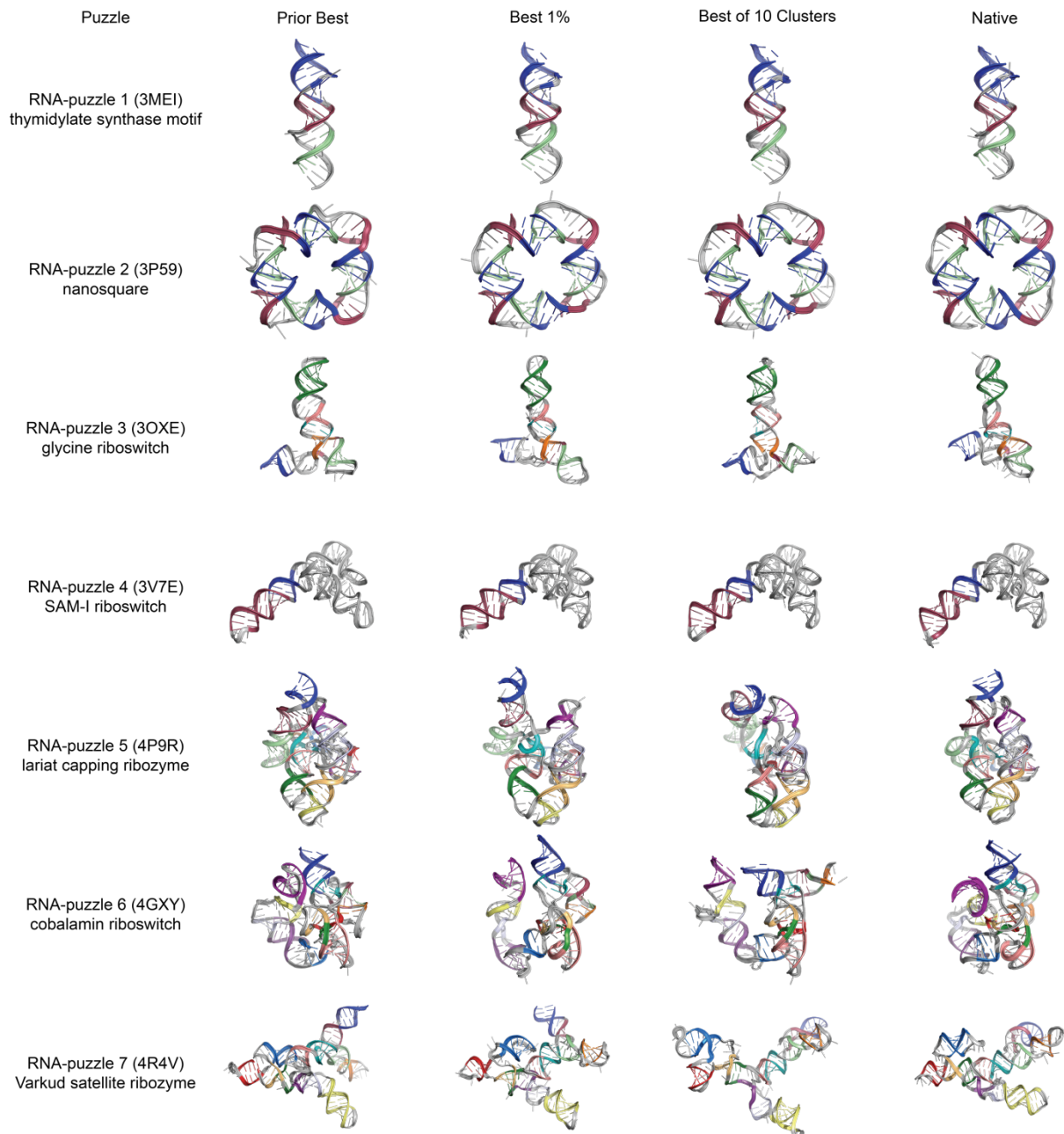
9

1



2

3 **Figure S2.** Related to Figure 1. FARFAR2 yields a superior RMSD to SWM among its five low-  
4 energy cluster centers in 44 of 82 benchmark cases. FARFAR2's particular advantage lies in  
5 cases where *both* SWM and FARFAR2 fail to obtain 1.5 Å RMSD accuracy: of the 6 cases  
6 where SWM provides worse than 5.0 Å RMSD, FARFAR2 provides a superior RMSD in 5. In  
7 contrast, among the 42 cases where SWM achieves better than a 1.5 Å RMSD, FARFAR2  
8 obtains superior RMSD in only 19.



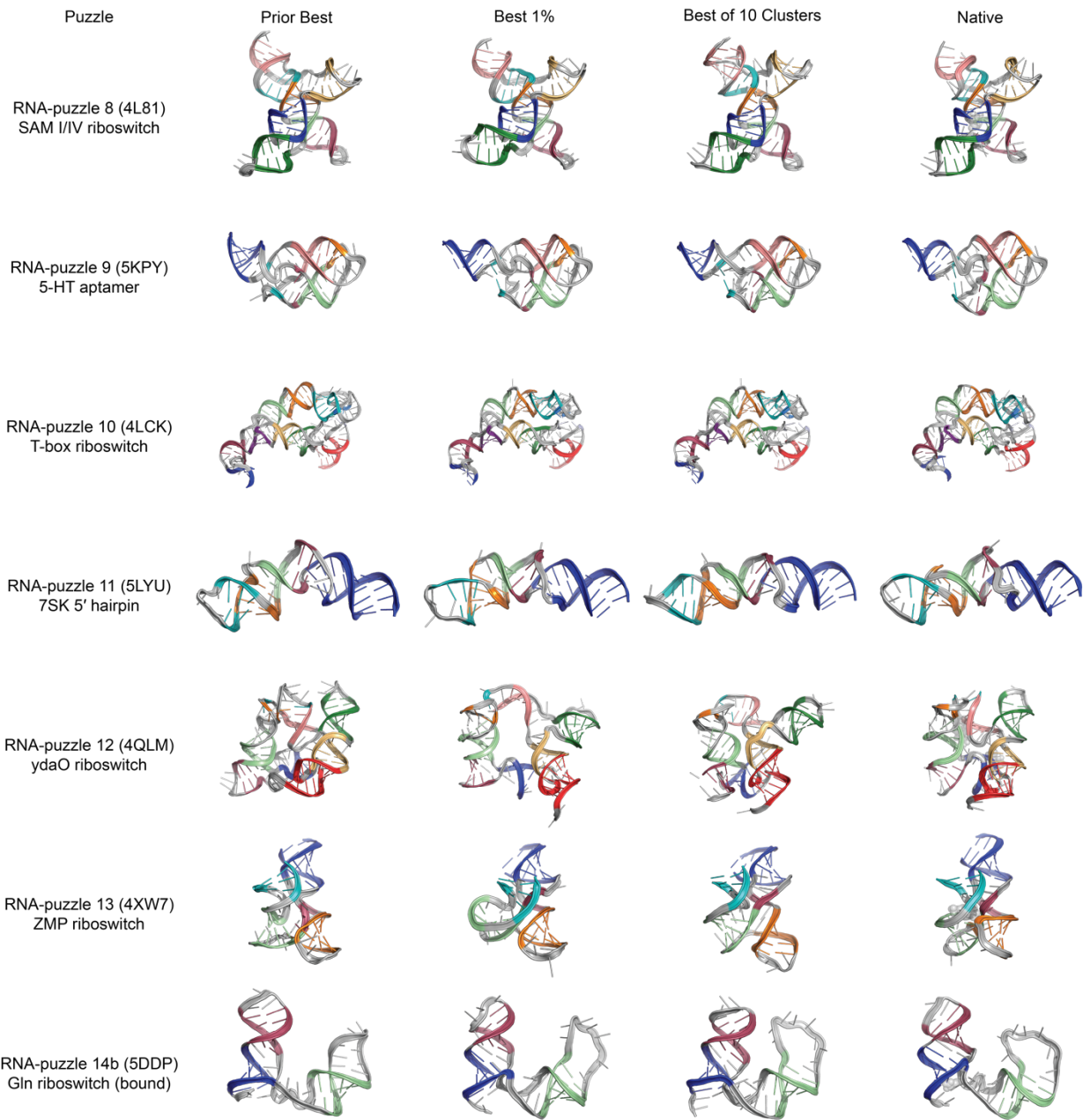
1

2 **Figure S3.** Related to Figure 3. Detailed depictions of FARFAR2-Puzzles benchmark cases 1-7,  
 3 including the best originally submitted model, the FARFAR2 model with lowest RMSD in the  
 4 top 1% of models overall, the lowest RMSD cluster center among the top 10 by energy, and the  
 5 native structure. Models are colored to highlight distinct secondary structure elements.

6

7

8



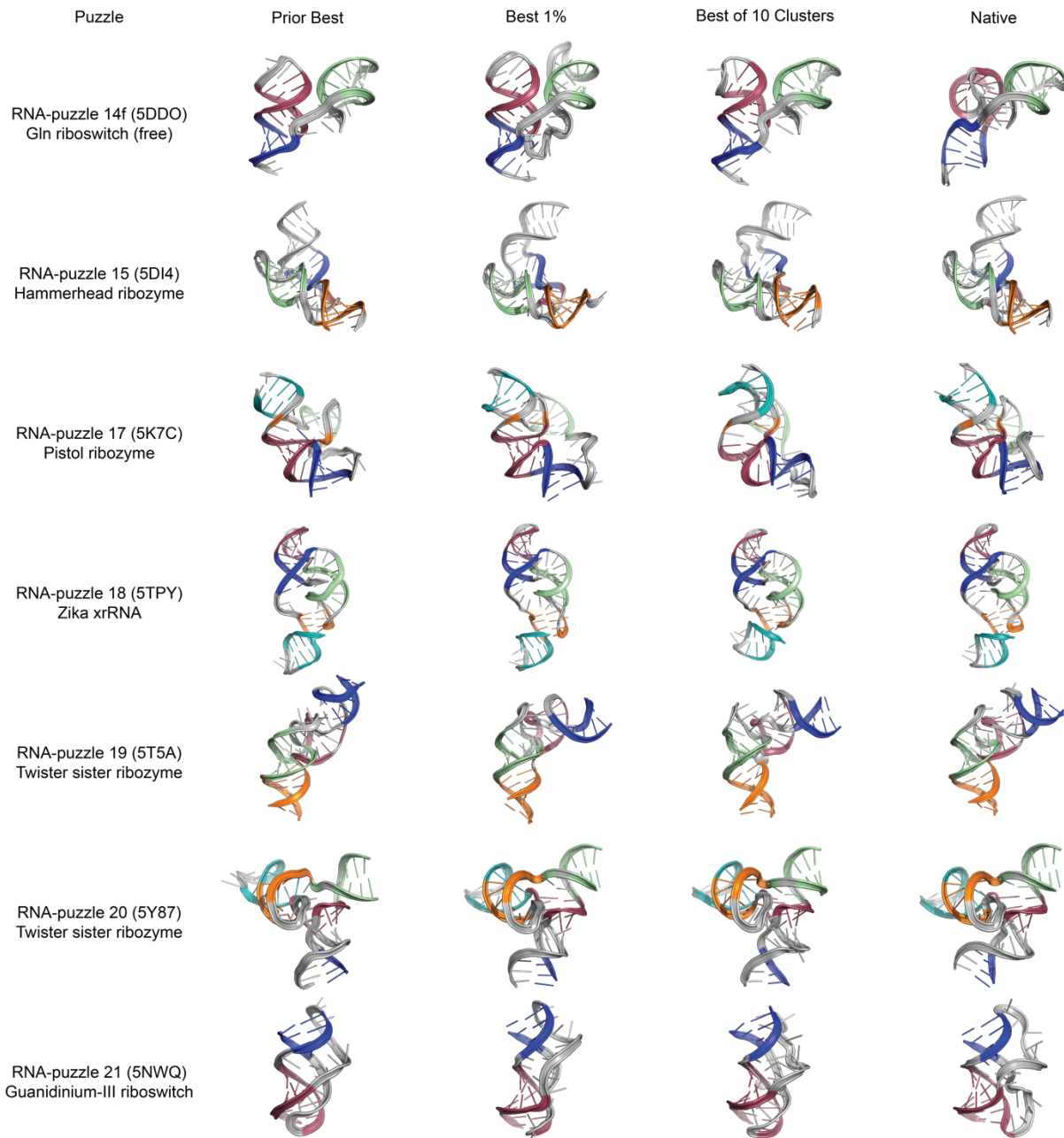
1

2 **Figure S4.** Related to Figure 3. Detailed depictions of FARFAR2-Puzzles benchmark cases 8-  
 3 14b, including the best originally submitted model, the FARFAR2 model with lowest RMSD in  
 4 the top 1% of models overall, the lowest RMSD cluster center among the top 10 by energy, and  
 5 the native structure. Models are colored to highlight distinct secondary structure elements.

6

7

8



1

2 **Figure S5.** Related to Figure 3. Detailed depictions of FARFAR2-Puzzles benchmark cases 14f-  
 3 21, including the best originally submitted model, the FARFAR2 model with lowest RMSD in  
 4 the top 1% of models overall, the lowest RMSD cluster center among the top 10 by energy, and  
 5 the native structure. Models are colored to highlight distinct secondary structure elements.

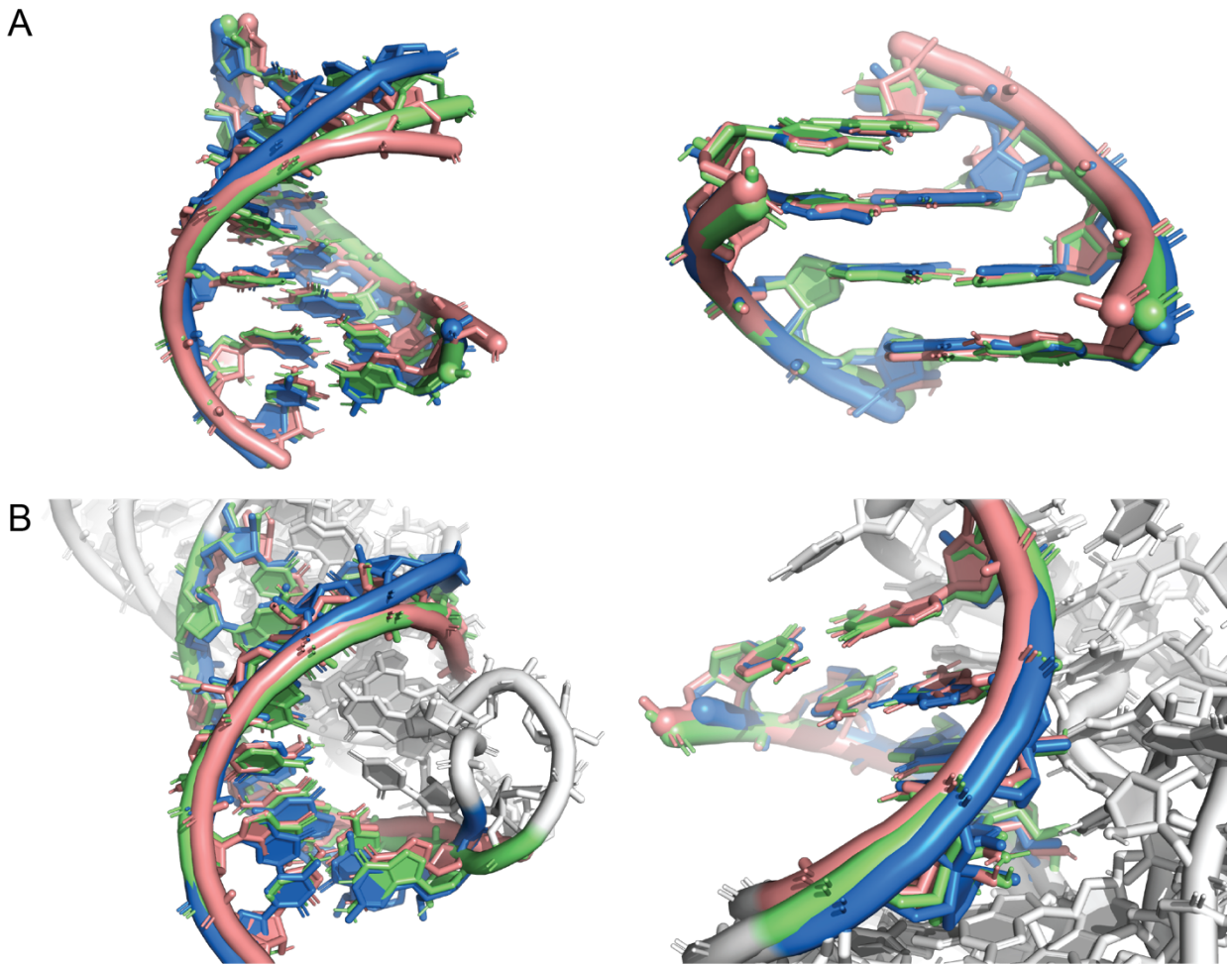


**Figure S6.** Related to Figure 5. Base pair steps provide the benefits of pre-generated helical ensembles. We conducted a detailed comparison of the performance of fixed helices versus base pair step sampling on both helices of RNA-Puzzle 21 (left and right). (A) We directly compared the two approaches for RNA-Puzzle 21 (native structures in blue). For both helices, fixed stems (pink) yielded a worse RMSD to the native helix conformation than base pair step sampling (green) ( $1.6 \text{ \AA} > 1.3 \text{ \AA}$ ;  $0.8 \text{ \AA} > 0.5 \text{ \AA}$ ). (B) These improvements represented geometrically important flexibility, when viewed in the context of the full structure: the tightly pseudoknotted structure of Puzzle 21 features no external stacking on either helix, and deviations from ideality are essential within each helix in order to relieve strain and achieve conformations where the helix termini have no residues stacked upon them.

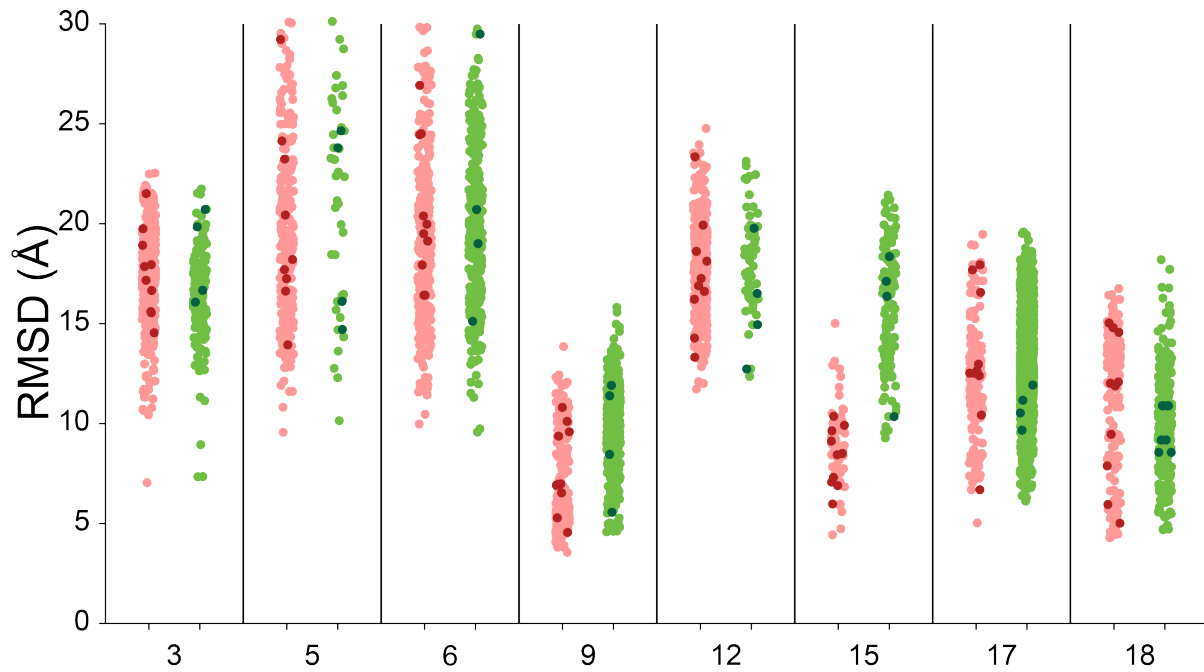


**Figure S7.** Related to Figure 5. A direct comparison of eight puzzles run with base pair step sampling (i.e., standard FARFAR2; pink points with red cluster centers) with an identical protocol using fixed helical stems (preserving the scoring function and fragment library; light green points with dark green cluster centers) confirms the utility of explicit sampling of helical flexibility.

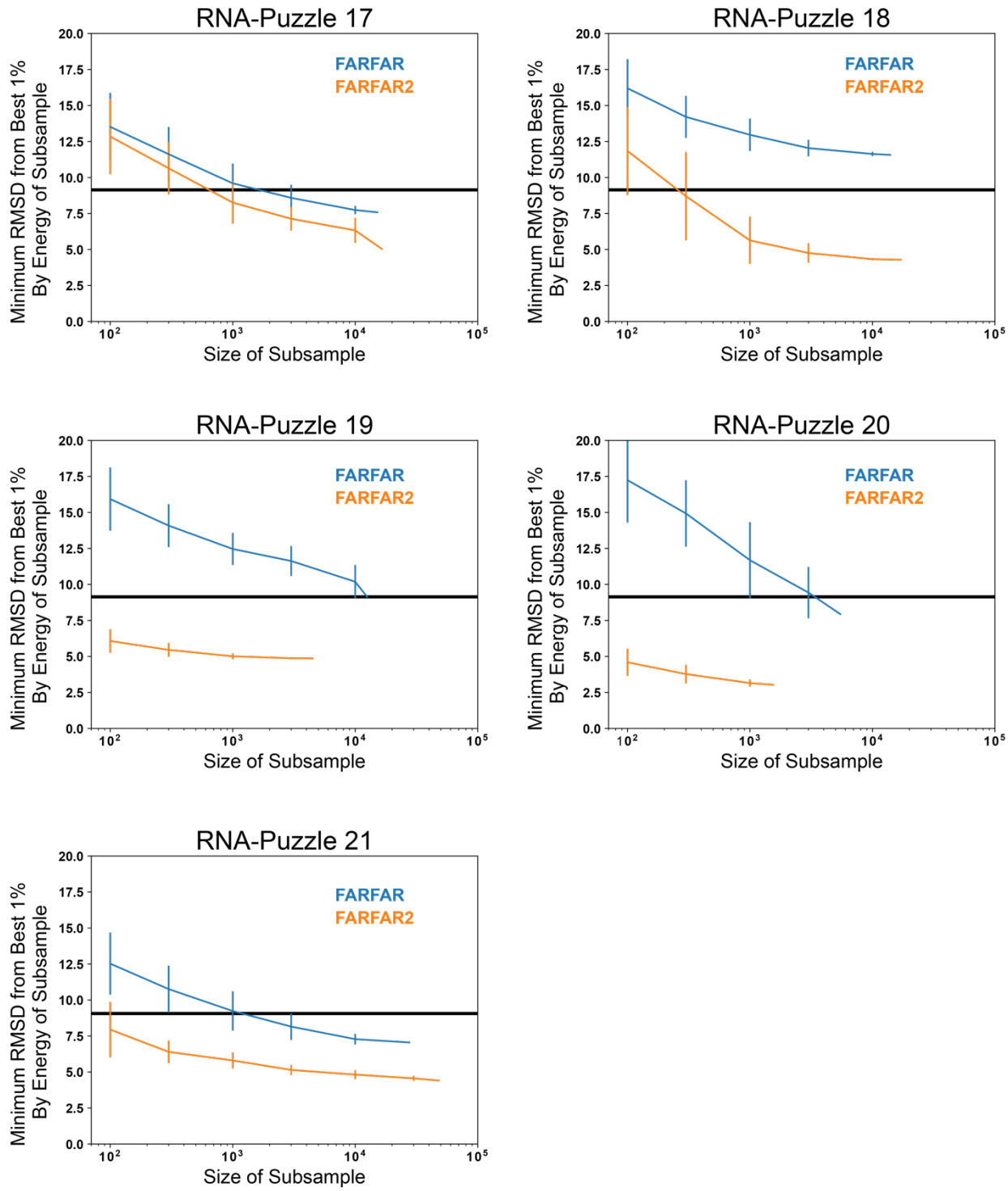


**Figure S8.** Related to Figure 3. Drawing subsamples from the respective model sets suggests that FARFAR2 (orange) begins to sample native-like ( $< 9.1 \text{ \AA}$ ) models within its lowest energy percentile more rapidly than a reproduction of original FARFAR with only base pair constraint inputs. The results are especially stark on structures with substantial structure from input

templates (RNA-Puzzles 19, 20, 21), but FARFAR requires 10x or 100x as many structures to obtain comparable results in the remaining cases as well.

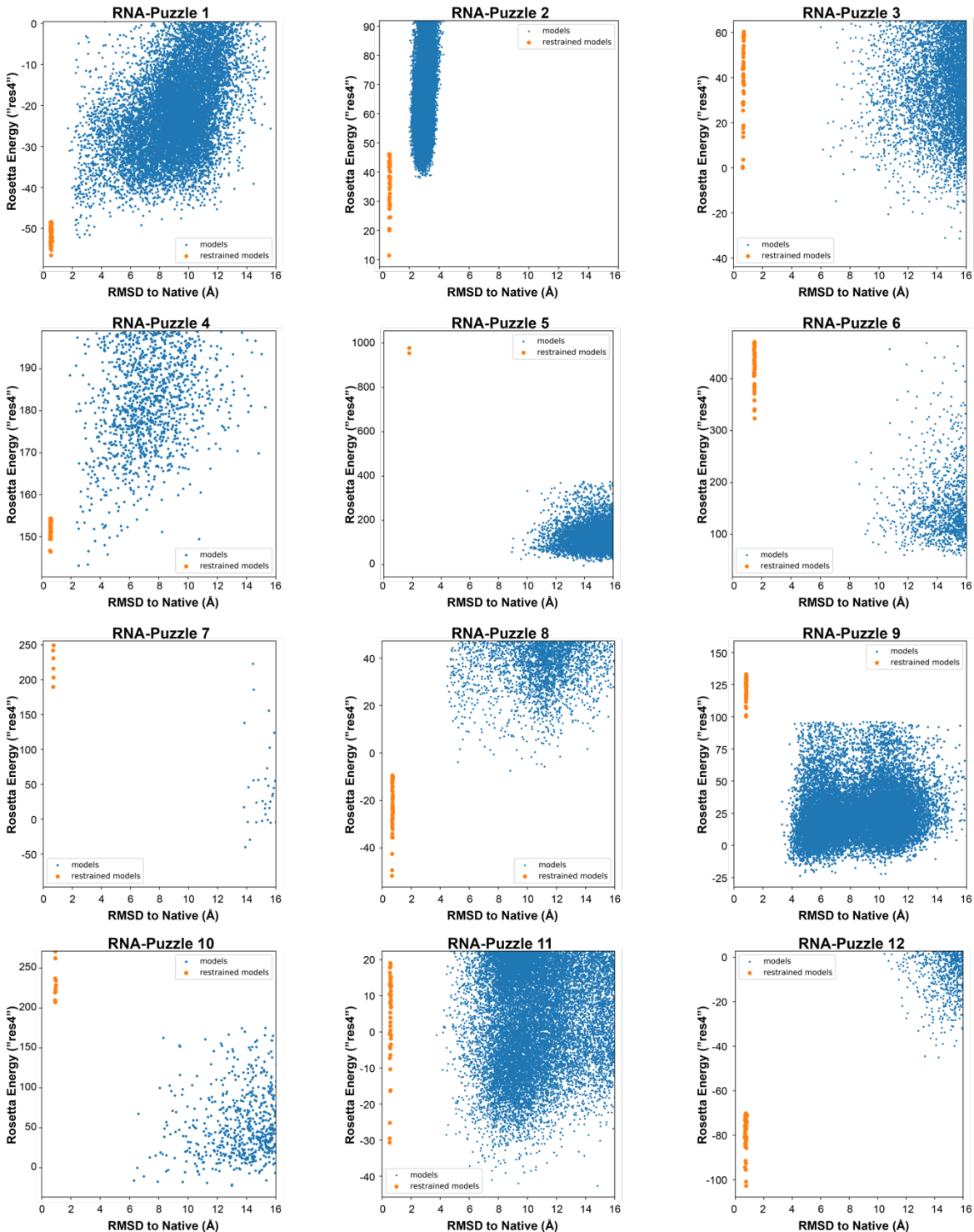


**Figure S9.** Related to Figure 3. For RNA-Puzzles 1-12, heavily restrained simulations (orange) forced to resemble the native reliably achieve sub-Ångstrom RMSDs, but often exhibit higher energies than the FARFAR2 model ensembles (blue).

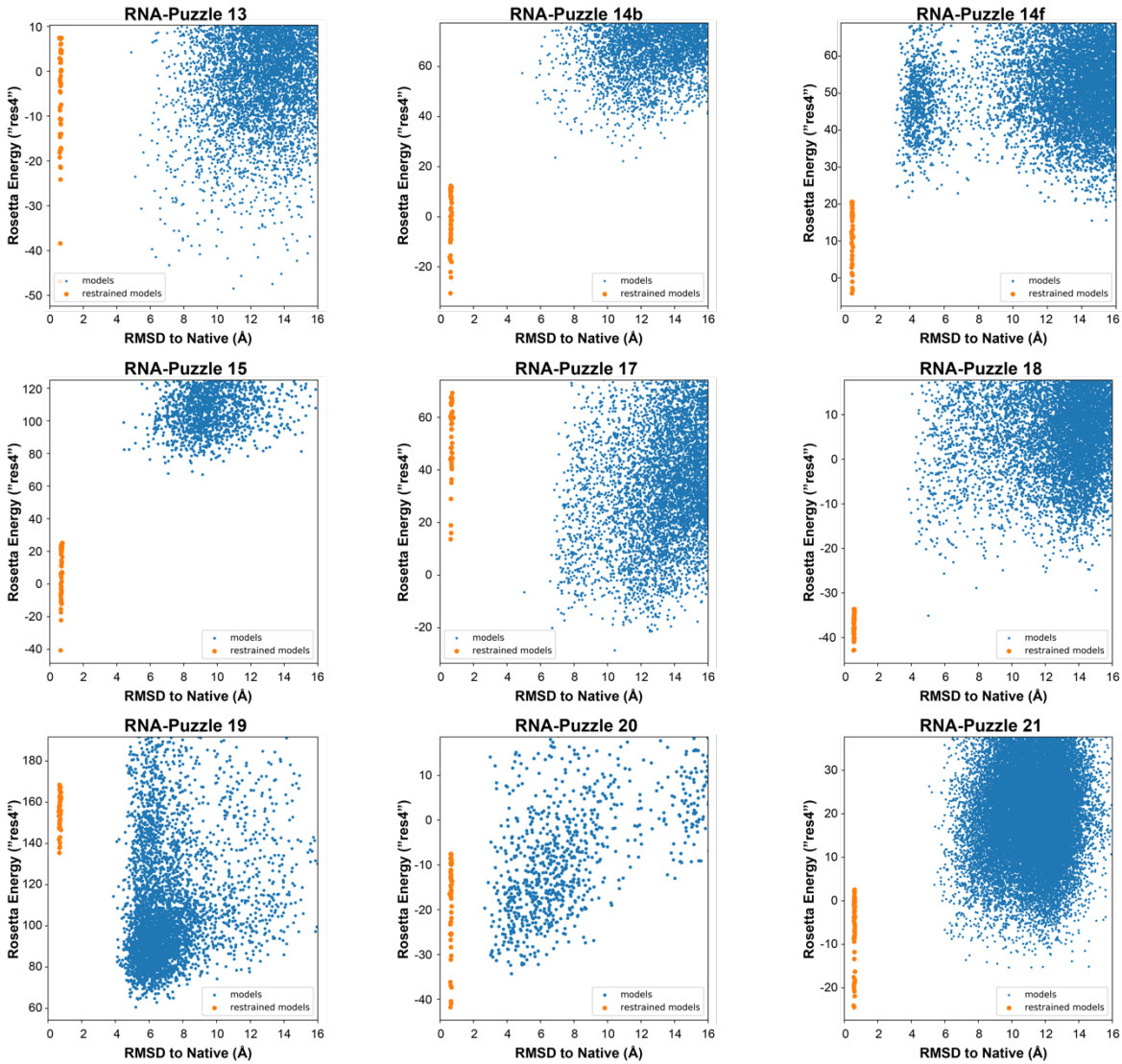


**Figure S10.** Related to Figure 3. For RNA-Puzzles 13-21, heavily restrained simulations (orange) forced to resemble the native reliably achieve sub-Ångstrom RMSDs, but often exhibit higher energies than the FARFAR2 model ensembles (blue).

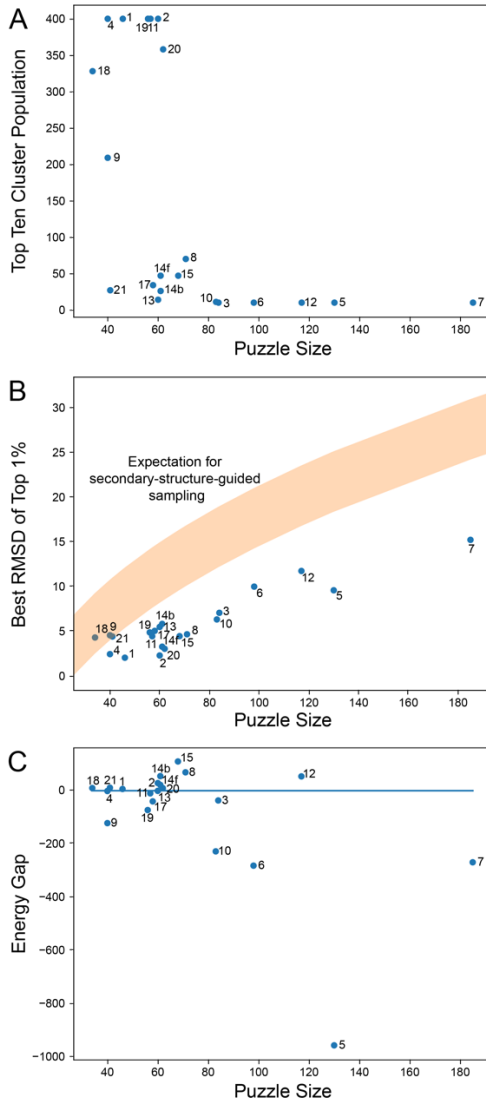


**Figure S11.** Related to Figure 3. (A) Larger puzzles tended to feature worse sampling, as judged by the total population of their top 10 clusters, though some smaller puzzles remain undersampled. (B) Nonetheless, across all puzzle sizes, the top 1% RMSDs from FARFAR2 simulations are superior to the threshold for a significant RNA structure prediction with specified secondary structure, which is given by the Weeks-Dokholyan power law relationship  $5.1 N^{0.41} - 15.8$ , where the shaded orange band represents a 95% CI (Hajdin, Ding, Dokholyan, & Weeks, 2010). (C) Larger puzzles also more often feature significantly positive or negative energy gaps.

**Table S1.** Related to Figure 1. Fragment assembly performance depends on multiple parameters optimized in this study. The performance of FARFAR2 (gauged by the lowest RMSD obtained from the 1% lowest energy models) was measured on the original FARNA benchmark to compare scoring functions, secondary structure input, fragment sets, and simulation guidance parameters. This study determined the ideal simulation parameters for use in the remaining larger-scale benchmarks.

1  
2

Fragment library	Old																New																New	New	New
	None		Fixed helix input				Secondary structure constraints				Base pair steps				None		Fixed helix input				Secondary structure constraints				Base pair steps				Base pair steps	Base pair steps	Base pair steps				
Mode of SS input	n/a	hires	rna4	n/a	hires	rna4	n/a	hires	rna4	n/a	hires	rna4	n/a	hires	rna4	n/a	hires	rna4	n/a	hires	rna4	n/a	hires	rna4	n/a	hires	rna4	n/a	hires	rna4	n/a	hires	rna4		
Minimization scoring function	n/a	hires	rna4	n/a	hires	rna4	n/a	hires	rna4	n/a	hires	rna4	n/a	hires	rna4	n/a	hires	rna4	n/a	hires	rna4	n/a	hires	rna4	n/a	hires	rna4	n/a	hires	rna4	n/a	hires	rna4		
157d	1.385	0.797	0.513	1.363	0.763	0.556	1.288	1.288	1.288	2.003	1.258	0.941	0.839	0.653	0.457	1.470	0.786	0.476	1.065	1.065	1.065	1.644	0.947	0.618	1.018	1.651	1.651	0.944	0.944	0.944	0.944	0.944	0.944		
1a4d	5.266	6.185	5.352	3.370	2.884	2.556	5.581	7.052	3.786	3.381	2.823	3.101	4.785	4.412	3.782	3.863	3.035	3.240	6.818	4.651	3.732	3.751	2.737	3.036	3.341	3.503	3.503	3.495	3.495	3.495	3.495	3.495	3.495		
1csl	2.472	2.275	1.814	2.303	3.133	1.956	2.160	2.160	2.160	3.004	3.066	2.508	2.021	1.971	2.297	2.323	2.399	1.914	1.639	2.094	1.639	2.592	3.341	2.368	2.592	2.164	2.164	2.164	2.273	2.273	2.273	2.273	2.273	2.273	
1dqf	0.968	0.699	0.972	0.704	0.708	0.791	1.064	0.938	1.087	1.028	1.029	0.933	1.621	1.242	1.072	0.699	0.768	1.159	1.645	1.842	1.810	0.929	0.989	0.666	0.772	0.726	0.726	1.226	1.226	1.226	1.226	1.226	1.226		
1esy	3.141	2.334	2.217	1.866	1.743	1.543	2.788	3.170	3.134	2.269	2.087	1.995	2.459	2.459	2.459	1.965	1.925	1.637	2.770	2.834	2.770	2.048	2.130	1.842	2.059	1.989	1.989	1.871	1.871	1.871	1.871	1.871	1.871		
1i9x	1.866	1.801	1.819	2.504	3.264	2.937	1.887	1.947	1.887	2.425	2.753	2.462	1.675	1.715	1.677	2.643	3.382	2.978	2.853	2.857	2.293	2.285	2.320	1.558	2.315	2.361	3.396	3.396	3.396	3.396	3.396	3.396			
1kd5	3.000	2.686	2.362	3.128	2.240	2.240	2.112	2.143	2.143	2.826	1.676	1.677	3.402	2.785	2.576	3.215	2.794	2.579	2.128	2.660	1.718	2.636	1.947	1.979	1.383	2.334	1.651	1.651	1.651	1.651	1.651	1.651			
1kka	3.785	3.546	3.546	5.233	5.263	5.210	3.603	3.688	3.482	3.262	3.111	3.377	3.888	3.739	3.486	5.155	5.090	5.223	3.616	3.531	3.413	3.215	3.331	3.252	3.693	3.579	3.493	3.493	3.493	3.493	3.493	3.493			
1l2x	2.415	2.935	9.981	2.255	2.302	2.410	2.715	2.885	2.715	2.270	2.996	2.664	2.261	2.360	8.813	2.293	2.196	2.276	2.449	2.922	2.922	2.434	2.483	2.763	3.414	2.727	2.499	2.499	2.499	2.499	2.499	2.499			
1mhk	7.539	6.591	6.639	5.770	4.458	5.079	6.451	4.264	4.310	3.668	3.848	4.305	5.114	4.921	5.204	5.473	5.195	4.835	6.988	6.409	6.505	5.809	4.556	4.735	4.780	6.025	4.716	4.716	4.716	4.716	4.716	4.716			
1q9a	4.156	3.645	4.082	4.013	4.111	4.173	3.954	3.869	3.954	4.085	2.178	3.248	4.184	4.144	4.184	3.989	2.298	4.024	4.295	4.448	4.448	4.008	3.234	3.217	1.581	4.067	4.091	4.091	4.091	4.091	4.091				
1qwa	3.378	3.293	3.733	2.747	2.928	3.136	3.291	3.456	3.344	2.869	3.480	4.005	3.613	3.345	2.911	2.928	2.652	2.863	3.328	3.397	3.328	2.358	2.729	3.375	2.967	2.793	3.840	3.840	3.840	3.840	3.840	3.840			
1xjr	12.32	9.913	9.919	7.659	6.623	6.694	8.115	7.520	6.531	7.127	6.352	6.270	11.00	9.254	8.636	5.848	4.950	7.057	8.375	7.141	7.130	7.178	7.241	7.012	7.197	7.815	5.855	5.855	5.855	5.855	5.855	5.855			
255d	1.354	1.282	1.296	1.556	1.146	1.078	1.221	1.234	1.234	1.488	1.517	0.982	1.339	1.173	1.249	1.237	1.070	1.160	1.208	1.208	1.162	1.155	1.201	1.135	1.016	1.290	1.290	1.290	1.290	1.290	1.290				
283d	1.651	1.780	1.702	4.086	1.163	1.305	1.566	1.469	1.714	1.746	1.865	1.717	1.723	1.443	2.357	4.993	1.167	1.226	1.619	1.516	1.879	2.548	1.572	1.337	1.623	1.684	1.361	1.361	1.361	1.361	1.361	1.361			
28sp	2.554	2.428	2.428	3.008	2.491	2.269	2.705	2.705	2.622	2.485	2.285	2.819	2.731	2.762	2.775	2.468	2.291	2.501	2.501	2.501	2.550	2.484	2.081	2.508	2.271	2.181	2.181	2.181	2.181	2.181	2.181				
2a43	6.679	6.701	5.399	3.326	3.341	3.055	3.973	3.973	3.598	3.250	3.155	3.448	3.919	4.063	3.767	3.176	3.069	2.859	3.100	3.100	2.986	2.722	2.839	3.556	3.807	2.468	2.468	2.468	2.468	2.468	2.468				
2f88	2.822	2.856	2.285	2.156	3.143	2.491	3.976	3.639	2.879	1.896	2.053	2.250	2.876	2.608	2.298	2.333	2.388	2.278	4.334	3.201	2.293	2.294	1.977	2.183	2.256	2.026	2.008	2.008	2.008	2.008	2.008	2.008			

3

1   **Table S2.** Related to Figure 1. Comparison of fragment assembly performance using the modern scoring function on the ‘motif-scale’  
2   benchmark set versus the performance of SWM on the same benchmark. More models were generated for the FARFAR version of the  
3   benchmark, but comparable computational time was required in each case. Unlike in the original SWM work, the relevant metric  
4   compared is the best RMSD sampled from among the 1% of models with the best energy.

5  
6

Benchmark Case	FARFAR	SWM	FARFAR	SWM
	1% RMSD (Å)	1% RMSD (Å)	Best of 5 Cluster RMSD	Best of 5 Cluster RMSD
<i>Trans-Helix Loops</i>				
5P_j12_leadzyme	2.56	0.82	2.56	1.22
5P_p1_m_box_riboswitch	2.64	2.13	2.68	0.63
3P_j55a_group_I_intron	0.27	1.72	0.42	0.40
5P_j55a_group_I_intron	3.28	3.25	3.87	0.74
hepatitis_C_virus_ires_IIa	3.23	3.11	3.47	2.56
j24_tpp_riboswitch	1.38	1.22	3.51	0.72
j23_group_II_intron	1.77	1.11	2.57	0.55
j31_glycine_riboswitch	5.53	0.54	5.53	0.65
11_sam_II_riboswitch	0.67	3.14	0.89	0.83
l2_viral_rna_pseudoknot	1.76	4.28	1.94	0.71
23s_rrna_44_49	1.20	0.71	1.23	1.25
23s_rrna_531_536	4.61	1.49	5.41	1.48
23s_rrna_2534_2540	1.97	7.28	2.90	6.94
23s_rrna_1976_1985	8.19	12.18	9.82	15.27
23s_rrna_2003_2012	7.54	9.85	9.85	9.02
Total cases: 15	6	9	3	12
<i>Apical Loops</i>				
gcaa_tetraloop	1.36	1.18	1.55	1.14
uuucg_tetraloop	2.57	2.29	2.03	1.14
gagua_pentaloop	0.75	2.94	0.76	1.10
anticodon_phe	1.30	2.82	2.21	2.24
Total cases: 4	2	2	2	2
<i>Two-Way Junctions, Fixed</i>				
puzzle1_alt_fixed	1.98	0.409	2.29	1.72
srp_domainIV_fixed	0.50	1.034	0.69	0.90
srl_fixed	0.54	0.707	0.69	0.56
kink_turn_fixed	0.80	2.02	1.28	1.45
j55a_P4P6_fixed	1.78	3.20	1.86	0.55
P5b_connect	0.76	3.63	0.76	2.68

gg_mismatch_fixed	1.87	0.32	2.03	0.32
tandem_ga_imino_fixed	1.07	0.86	1.21	0.87
tandem_ga_sheared_fixed	0.37	0.61	0.50	0.61
hiv_rre_fixed	0.36	0.87	0.45	0.35
j44a_p4p6_fixed	0.75	0.56	1.03	0.58
just_tr_P4P6_fixed	0.66	0.63	0.68	0.61
r2_4x4_fixed	0.72	1.44	1.20	1.49
loopE_fixed	0.51	1.74	0.72	1.74
<i>Total cases: 14</i>	<i>9</i>	<i>5</i>	<i>6</i>	<i>8</i>
<i>Three-Way Junctions, Fixed</i>				
hammerhead_3WJ_cat_fixed	3.25	1.62	3.71	3.05
hammerhead_3WJ_precat_fixed	1.16	1.60	1.90	1.57
VS_rbzm_P2P3P6_fixed	0.76	0.74	1.09	0.57
VS_rbzm_P3P4P5_fixed	1.21	1.91	1.21	1.91
hammerhead_3WJ_cat_OMC_fix ed	2.85	2.16	4.56	3.04
<i>Total cases: 5</i>	<i>2</i>	<i>3</i>	<i>1</i>	<i>4</i>
<i>Tertiary Contacts, Fixed</i>				
tl_tr_P4P6	0.55	1.07	0.55	0.64
hammerhead_tert_fixed	0.96	2.45	1.00	1.16
kiss_add_fixed	2.28	3.24	2.69	2.40
kiss_add_L2_fixed	0.52	1.50	0.69	0.71
kiss_add_L3_fixed	1.42	2.11	1.57	0.88
puzzle18_zika_PK	2.67	2.01	2.67	1.97
gir1_p2.1p5_kiss_fixed	1.19	1.94	1.62	1.99
gir1_p2p9_gaaa_minor_fixed	0.83	2.02	1.02	1.58
t_loop_fixed	0.78	2.27	0.78	0.95
t_loop_modified_fixed	2.37	1.24	0.98	1.33
<i>Total cases: 10</i>	<i>8</i>	<i>2</i>	<i>7</i>	<i>3</i>
<i>Two-Way Junctions, Aligned</i>				
gg_mismatch	1.12	2.65	1.12	0.79
tandem_ga_imino	0.89	1.32	1.03	0.98
tandem_ga_sheared	0.49	1.06	0.61	0.75

hiv_rre	1.78	3.59	1.94	2.12
j44a_p4p6	1.01	4.75	1.56	1.59
just_tr_P4P6	0.74	2.47	0.96	1.22
cg_helix	0.23	0.63	0.28	0.58
puzzle1	0.91	3.26	0.84	0.96
srp_domainIV	0.94	2.88	1.01	1.26
r2_4x4	1.84	3.34	1.84	1.74
gagu_forcesyn_blockstackU	4.65	5.64	4.87	4.49
srl_free_bulgedG	4.59	6.38	4.76	4.66
j55a_P4P6_align	0.85	2.81	1.04	2.04
kink_turn_align	0.79	3.01	0.97	2.07
loopE	0.91	5.28	1.75	2.00
<i>Total cases: 15</i>	<i>15</i>	<i>0</i>	<i>10</i>	<i>5</i>
<i>Three-Way Junctions, Aligned</i>				
hammerhead_3WJ_precat	2.83	10.74	4.18	6.09
VS_rbzm_P2P3P6_align	0.73	1.29	0.84	1.13
VS_rbzm_P3P4P5_align	1.04	2.40	1.86	2.60
hammerhead_3WJ_cat_OMC_ali	2.56	2.89	4.22	2.89
gn				
puzzle18_zika_3WJ_extraminres	2.52	4.36	2.99	2.42
<i>Total cases: 5</i>	<i>5</i>	<i>0</i>	<i>3</i>	<i>2</i>
<i>Tertiary Contacts</i>				
gaaa_minor_dock	1.02	2.26	1.19	1.41
gir1_p2.1p5_kiss	1.48	3.25	2.01	2.75
gir1_p2p9_gaaa_minor	1.17	2.60	1.16	1.83
tl_tr_P4P6_dock	0.81	6.83	0.81	3.03
kiss_add_PK_dock	2.07	3.46	3.35	2.58
t_loop_align	2.02	4.16	2.02	3.20
hammerhead_tert_align	3.08	7.87	3.90	8.65
t_loop_modified_align	1.93	3.66	2.44	3.99
<i>Total cases: 8</i>	<i>8</i>	<i>0</i>	<i>7</i>	<i>1</i>
<i>Non-Helix Embedded</i>				
cg_helix_Zform	5.00	10.76	5.00	1.75

g_quadruplex_fixed	1.58	3.57	1.79	2.75
g_quadruplex_inosine_fixed	1.84	2.43	2.03	2.87
bru_gag_tetraplex	3.30	2.78	2.70	3.42
parallel_AA	0.97	1.22	<b>1.16</b>	<b>1.41</b>
bulged_tetraplex	4.95	7.67	<b>5.04</b>	<b>7.37</b>
<i>Total cases: 6</i>	<i>5</i>	<i>1</i>	<i>5</i>	<i>1</i>
<i>Overall: 82</i>	<i>60</i>	<i>22</i>	<i>44</i>	<i>38</i>

1

**Table S3.** Related to Table 1. Exact inputs (sequence and RNA templates) used in modeling for each RNA-puzzle problem.

9	ggcacacugauauggcacgcauugaauuguuggacaccguaaaugucc aacacgugucc ((((((.....(((((.....[[)))))))).....((([].....)))).....))))	Template structures from original Das lab modeling: kissing loop from 2XNW; T-loop from the tRNA Phe structure 3L0U.
10	ugcgaugagaagaagaguauuaaggauuuacuauagcgacucuaggauagugaaag cuagaggauaguaaccuuuagaaggcacuucgagca, aguaguucagugguagaacacca ccuugccaaggugggggugcgcggguicgaaucuccgucu (((((.....(((((.....(((((.....(((((.....(((((.....))))))))....))))))))....[[[.]]))))....), ((..(((.....{.}))..(((..[]])..))))....(((..}.....))))....)	Template structures from original Das lab modeling: a kink-turn from 2GIS provided A:1-10, A:90-96; a loopE motif from 5S rRNA 354D furnished A:16-20, A:80-83; a double T-loop motif from 4JRC supplied A:37-43, A:53-60; and part of a tRNA from 2K4C delivered B:6-18, B:20-3,0 B:38-66.
11	gggaucugucaccccacauugaucgcuucgggcugaucuggcuggcuaggcgccc ((((((...(((((.....(((((.....))))....))))....))))....)))	Just secondary structure
12	gaucgcugaacccga, aggggcgggggacccag, ggggcgaauucucuuccgaaaggaga guaggguuacuccuucgaccgcagccgcugcagcuaaccucgcagcgcuuccgaaaggagaa ....(((((.....((.,.))))(((((.....(.,(((((.....(((((.....))))))..(((((.[[[[[[.]]))))....))))....))))....))))....)]])..	Just secondary structure
13	gggucgugacuggcgaacaggugggaaaccaccggggagcgaccc, gcccggccuggg c ((((((...(([[[[. ....(((((.....))))....))))....))))....([[[.]]]..)))	Just secondary structure
14b	cguugacccaggaaacuggcggaaguaaggccauugcacuccggccugaagcaacgc g (((((.(((((.....)))).....(((((.....))))....))))....))))....	Just secondary structure (original puzzle omits U1A loop in RMSD calculations)
14f	cguuggccaggaaacugggu, aguaaggcccacuugcacuccggccugaagcaacgc (((((.....))))....(((((.....))))....))))....)	Just secondary structure (original puzzle omits U1A loop in RMSD calculations)
15	ggguacuaagccacugauagagucgcugggaugcgcacgaaacgcca, gggcgugcagg caguaccca .....(((((.....(((((.....))))....(((((.....))))....))))....)))	Just secondary structure
17	cgggguaagggccacguuaauaguugcuaagccuaagcguugau, aucaggugcaa (((([[[[.]])))).....(((((.....]]]))....((.,.))))....)))	Just secondary structure
18	gggcacggccggcgaagucgccacaguuuggggaaagcugugcagccuguaacccccc acgaaaguggg ....(((((.....))))....(((((..[[[.]]))))....))))....]]])((((.....))))	Template structures from original Das lab modeling from 4PQV.
19	gcaggggcaaggcccacucccgugcaagccgggaccggcccc, ggggcgcggcgcucauucc ugc ((((...(((((.....))))....(((((.,))))....))))....)))	Template structures from original Das lab modeling: threaded T-loop from 1B23, with intercalating A:8 modeled in. (Other suspected intercalators like A:9 and B:15 score strictly worse.)
20	acccgcaaggcccacggc, gccgcgcugugugcaaguccacgcuucggcgugggcg cucaugggu	Template structures from original Das lab modeling: threaded T-loop from puzzle 19 (5T5A), renumbered.

	<pre>(((((...((((((.,))))).((((.....))))(((((....))))))). ))....)))</pre>	
21	<pre>ccggacgaggugcgccguaccggucaggacaagacggcgc [[[[.....(((((..]]].....))))]])</pre>	Just secondary structure, no guanidinium.
1		
2		

1   **Table S4.** Related to Table 1. Comparison of performance between a reproduction of FARFAR original modeling conditions (where  
2   secondary structure was modeled using base pair constraints) versus FARFAR2.  
3

Puzzle	FARFAR2 Top 1% Best RMSD	FARFAR2 Best of 10 Cluster RMSD	FARFAR Top 1% Best RMSD	FARFAR Best of 10 Cluster RMSD
17	5.03	6.69	7.58	11.43
18	4.29	5.02	11.57	11.78
19	4.86	5.16	9.14	13.44
20	3.03	4.03	7.94	7.94
21	4.40	6.04	7.05	10.26

4  
5

1 **Table S5.** Related to Table 1. Energy gaps between the minimum energies sampled in artificially restrained near-native simulations  
 2 and FARFAR2 models for each FARFAR2-Puzzles benchmark case. A positive energy gap indicates that the best energy achieved in  
 3 FARFAR2 *de novo* modeling is higher (worse) than the energy observed for near-native conformations; a negative energy gap  
 4 indicates that the best energy from the FARFAR2-Puzzles benchmark is also the best energy overall. The total population in the top 10  
 5 clusters (maximum: 400) also indicates whether the benchmark case was thoroughly sampled.  
 6

Puzzle	RNA	Energy Gap	Total Top 10 Cluster Population
1	thymidylate synthase motif	4.4	400
2	nanosquare	26.6	400
3	glycine riboswitch	-38.7	10
4	SAM-I riboswitch	-3.3	400
5	lariat capping ribozyme	-958.5	10
6	cobalamin riboswitch	-283.6	10
7	VS ribozyme	-270.9	10
8	SAM I/IV	67.0	70
9	5-HT aptamer	-123.8	209
10	T-box riboswitch	-229.9	11
11	7SK 5' hairpin	-12.0	400
12	ydaO riboswitch	51.7	10
13	ZMP riboswitch	-2.7	14
14b	Gln riboswitch (bound)	52.7	26
14f	Gln riboswitch (free)	19.6	47
15	hammerhead ribozyme	107.7	47
17	pistol ribozyme	-42.2	34
18	Zika xrRNA	7.8	328
19	twister sister ribozyme	-74.8	400
20	twister sister ribozyme	7.5	358
21	guanidinium-III riboswitch	9.1	27

1 **Table S6.** Related to Table 1. Detailed results for each RNA-Puzzle challenge revisited in this work.

Puzzle	FARFAR2 Top 1% Best by RMSD <sup>†</sup>			FARFAR2 Best of 10 Cluster by RMSD <sup>†</sup>			Best RNA-puzzle RMSD (All Submissions) <sup>‡</sup>		
	RMSD	F <sub>NWC</sub>	Clashscore*	RMSD	F <sub>NWC</sub>	Clashscore	RMSD	F <sub>NWC</sub>	Clashscore
1	2.03	0.90	2.72	2.50	0.86	4.07	3.40	0.90	0.00
2	2.28	0.00	11.31	2.71	0.00	10.99	2.30	0.50	14.23
3	7.05	0.11	4.79	12.41	0.00	2.58	7.60	0.22	0.00
4	2.43	1.00	22.16	2.52	1.00	19.69	3.40	0.88	1.97
5	9.57	0.25	3.64	13.94	0.26	2.32	9.58	0.20	9.93
6	9.98	0.20	7.82	13.08	0.20	10.35	12.28	0.27	27.88
7	15.21	0.00	5.72	18.52	0.14	2.69	20.72	0.50	11.25
8	4.65	0.50	10.27	5.23	0.75	5.45	4.80	0.75	13.77
9	4.54	0.64	2.64	4.56	0.50	1.76	5.86	0.29	18.53
10	6.31	0.70	5.54	6.31	0.65	5.54	6.78	0.70	13.82
11	4.43	0.00	0.55	6.04	0.14	1.10	5.22	0.00	0.55
12	11.73	0.15	3.71	13.32	0.23	4.24	10.15	0.00	12.61
13	5.47	0.00	7.73	7.13	0.67	6.19	5.41	0.33	10.85
14b	5.81	0.00	6.61	6.88	0.00	4.06	5.79	0.50	11.65
14f	3.26	0.67	7.00	11.85	0.00	3.23	6.05	0.83	16.24
15*	4.44	0.75	8.24	5.98	0.75	6.40	5.30	0.50	5.91
17	5.03	0.00	3.24	6.69	0.00	2.16	7.13	0.11	6.53
18	4.29	0.33	3.92	5.02	0.50	4.79	3.15	1.00	0.43
19	4.86	0.67	15.07	5.16	0.67	11.52	5.50	0.33	18.97
20	3.03	0.67	3.21	4.03	0.67	2.75	6.80	0.33	37.37
21	4.40	0.00	4.52	6.04	0.00	0.75	3.93	0.11	13.53

2 \*Clashes may come from input template structures that were not employed in the previously submitted modeling.

3 †Heavyatom RMSD is calculated over all residues, following superposition over all residues.

4

**Table S7.** Related to Table 2. Exact inputs (sequence and RNA templates) used in modeling for each blind challenge modeled in this work.

Blind challenge	Secondary Structure	Inputs
<i>F. nucleatum</i> glycine riboswitch	ucggauagaagauaugaggagagauuucauuuuuaugaaacaccgaagaag uaaucuuucagguaaaaaggacucauauuggacgaccucucugagagcu uaucuaaggagauaacaccgaaggagacaaagcuaauuuuagccuaaacucu cagguaaaaaggacggag ((.....((((((.....((((((.....)))))).(((.....((..... .....)))).....))).((((.....((.....)))).....))).(((.....(( ((.....))))).(((.....((.....((.....)))).....))).((.....))..... ))).....)))	3P49 furnished residues A:19-29 A:34-71 A:92-164.
<i>V. cholerae</i> glycine riboswitch	uccguugaagacugcaggagaguguuuuaaccagauuuuaacaucuga gccaaauaaccgcgcgaagaaguuaaucuuucaggugcauuuuucuuagc cauauauuggcaacgaaauagcgaggacuguaguuggaggaaccucugga gagaaccguuuuaucggucgcgcgaaggagcaagcucugcgcauauugcaga gugaaacucucaggcaaaaggacagagaga [[[.....((((((.....((((((.....)))).....)))).....)). .....))).(((.....((.....)))).....))).(((.....((..... ((.....)))).....))).(((.....((.....((.....)))).....))). .....))).(((.....((.....((.....)))).....)))......]]....((((.. ..((.....)))).....))).(((.....((.....((.....))))..... )).....)))......))....)))	Threaded template from lowest energy model of <i>F. nucleatum</i> glycine riboswitch modeling above: residues A:1-29 A:34-64 A:68-91 become A:1-29 A:56-86 A:125-148.
<i>Mycobacterium</i> SAM-IV riboswitch	gguaugagugccagcgucaagccccggcuiugcuggccggcaaccucca accgcgguggggugcccccggugaccaaggugaguagccgugacggc uacgcggcaagcgcggguc ((((.....(((((.....((.[[[[[.)))))))))).((..(((((.((. .{{(.))))..))))..))))]]....))).((((.(((((.....) ))))..)))......}}})...	SAM binding site from 2YGH provided A:1-9 A:38-43 A:63-66 A:76-79, with SAM as B:120
<i>G. kaustophilus</i> T-box riboswitch/tRNA-Gly	gcggaauguauucagugguagaacaccaccuugccaaggugggggugcgcg gguucgaauccccgcuuccgcucca, gaaaguggggugcgcguuuggcgcaucaacucggguggaaccgcgggagcu acgcucucgcucccgag ((((.....(.....(.....(.....))))[[[., .....(((((.....))))....))).....(((.]]]....(((..... .....))))....))))..	Threaded tRNA template from 4LCK: residues B:6-66
<i>B. subtilis</i> T-box riboswitch/tRNA-Gly	gcggaauguauucagugguagaacaccaccuugccaaggugggggugcgcg gguucgaauccccgcuuccgcucca, guugcagugagagaaagaaguacuugcguuuaccucaugaaagcgaccuu agggcgcgguaagcuaaggaaugagcacgcacaaaggcauucuugagca auuuuuaaaaagaggcugggauuuuuguucucagcaacuaggugggugaaaccg cgggagaacucucgcuccua ((((.....(.....(.....(.....))))[[[., .....(((((.....(((((.....(((((.....((.....))))....))))....))))	Threaded tRNA template from 4LCK: residues B:6-66; threaded T-box template from 4LCK: residues A:2-12 A:19-29 A:34-74 A:76-84 A:87-89 A:94-101

	).....((((((.....))))))...(((([]])...(((((....))))))))	
VA RNA I	ggaccucgcaaggguaucauggcgacgaccgggguucgaaccccggauc cggccgcuccgccugauccaugcgguuaccgcccgcugucgaacccagg ugugcgaggucc (((((((((.((((.(((((((((.((((.((.((.....))))))) ))))))))))))...((((((..[[[.))))....))))....))))..]] .))))))))	Just secondary structure

1

2